

1           **Modular bioelectrochemical wetland: A demonstration**  
2                           **study for treating urban wastewater**

3           Ting Wei<sup>1,2</sup>, Manuel E. López Sepúlveda<sup>3</sup>, Silvia Blázquez Hernández<sup>1</sup>, Lorena

4                           Peñacoba-Antón<sup>3</sup>, Yaqian Zhao<sup>2</sup>, Abraham Esteve Núñez<sup>1,4\*</sup>

5           <sup>1</sup>, *Universidad de Alcalá, Chemical Engineering Department, Alcalá de Henares,*

6           *Madrid, Spain*

7           <sup>2</sup>*State Key Laboratory of Eco-Hydraulics in Northwest Arid Region, Xi'an University*

8           *of Technology, Xi'an 710048, P.R. China*

9           <sup>3</sup>*METfilter, Madrid, Spain*

10          <sup>4</sup>*IMDEA WATER, Alcalá de Henares, Madrid, Spain*

11          

---

  
12          \* *Corresponding author: Abraham Esteve Núñez: [abraham.esteve@uah.es](mailto:abraham.esteve@uah.es)*

13  
14          **Abstract:**

15          The integration of microbial electrochemical technologies (MET) into treatment  
16          wetland (TW) led to a new generation of nature-based solution so-called METland<sup>®</sup>. In  
17          this context, METland<sup>®</sup> concept was further expanded to modular METland<sup>®</sup> while a  
18          comprehensive evaluation of a demo scale is reported for the treatment of real domestic  
19          wastewater. The overall treatment system included the following METland biofilter  
20          configurations: i) a horizontal flow modular unit, ii) a downflow unit made of EC coke,  
21          and iii) a downflow unit made of EC biochar. This hybrid treatment system aims to  
22          enhance pollutant removal efficiency through MET, leveraging the conductive

23 properties of substrates to optimize microbial metabolic processes. The system  
24 exhibited high COD removal efficiency (>90%) regardless of high feeding rate (ca.  
25 0.5m<sup>3</sup>/m<sup>2</sup>day) and significant nitrogen removal, with the ECBB unit showing high  
26 ammonia removal efficiency (90%). Standard treatment wetlands do not incorporate  
27 tools for monitoring the *in situ* performance of the systems. However, the  
28 electrochemical nature of the METland<sup>®</sup> allows continuous monitoring by measuring  
29 electrochemical parameters. In this context, electric potential (EP) measurements  
30 revealed spatial variations in electron utilization within the wetland, correlating with  
31 pollutant degradation. The electron current density (J=43.99 mA/m<sup>2</sup>) within the system  
32 decreased along the flow path, indicating a consistent electrochemical activity aligned  
33 with the treatment process. High correlations between J values and COD concentrations  
34 suggest the potential use of electrochemical indicators as proxies for pollutant levels in  
35 wastewater treatment. This study gives insights into the electrochemical behaviour of  
36 the system to provide a foundation for future optimization.

37 **Keywords:** Modular constructed wetland; urban wastewater; electrobioremediation,  
38 METland, Microbial electrochemical technology; Electroconductive substrates

39

## 40 **1 Introduction**

41 Recent studies about water scarcity indicate that half of the world's population will live  
42 in water-stressed areas very soon. Thus, in this scenario there is an urgent need develop  
43 decentralized wastewater systems capable of generating reclaimed water ready to be  
44 used [1]. In this context, treatment wetlands (TWs), also known as constructed wetlands

45 (CW), are a nature-based and cost-effective solution capable of treating wastewater by  
46 using a biofilter inspired by natural elements (gravel, plants and microorganisms) [2–  
47 5]. The core of the treatment wetland is the bed material, so researchers and engineers  
48 in recent years have sought and tested various innovative substrates to elevate pollutant  
49 removal efficacy in TW systems [6–8].

50 Among all materials, the use of those with electroconductive nature triggered the  
51 born of a new variety of TW where electromicrobiology concepts are integrated with  
52 the purpose of boosting biodegradation or harvesting energy [9–11]. Thus, electrodes  
53 can be allocated into classical TW inert beds to generate electrical energy from  
54 microbial metabolism of organic pollutants as part of devices so-called microbial fuel  
55 cells (MFCs) [12,13]. Actually, the new generation of TW capable of generating energy  
56 is named TW-MFC [14,15]. According to the previous studies, the range of  
57 bioelectricity power generation by various TW-MFCs is approximately 0.11-452.24  
58 W/m<sup>2</sup> [16–18]. Alternative to power production, other researchers have merged  
59 electrochemistry and TW in a very different scenario where classical electrochemical  
60 terms like anode and cathode were replaced by the use of a single electroconductive  
61 material operated as microbial electrochemical snorkel. Indeed, the new configuration  
62 so-called METland was conceived after replacing all inert material such as gravel by  
63 electroconductive granular material [19,20]. Among materials used in the METland  
64 bed, authors have mainly reported conductive coke [19,21] or more sustainable  
65 materials such as conductive biochar obtained after high-temperature pyrolysis of wood  
66 [22–24]. In addition to its conductive nature, electroconductive biochar can also exhibit

67 substantial electron storage capacities, thanks to their redox moieties acting act as a  
68 redox buffer when there is limited availability of electron donors or acceptors [25].  
69 Thus, regarding materials two different mechanisms can be identified in METland:  
70 geoconductor mechanism and geobattery mechanism [23]. The current understanding  
71 of how electroactive microbial communities operate in METland suggests that  
72 microbial extracellular electron transfer, either in form of DIET (Direct Interspecies  
73 Electron Transfer) [26] or CIET (Conductive-particle-mediated Interspecies Electron  
74 Transfer) [27,28], eventually, allow interconnection between microbial communities  
75 through the role bacteria from *Geobacter* genus, obtaining optimal synergies leading to  
76 efficient removal from wastewater [10,29,30].

77 Moreover, the microbial electrochemical activity inside METland was  
78 demonstrated by measuring electrochemical parameters like electric potentials (EPs)  
79 and electron current density, allowing the operator to monitor the performance and  
80 efficiency of the process in real time [21–23,31].

81 Constructed METlands followed similar design methods to traditional TWs.  
82 Indeed, they have been applied under different environmental and operating conditions  
83 in diverse geographic regions while achieving COD removal efficiencies of ca. 90%  
84 [31] including emerging pollutants [32]. Furthermore, a life cycle assessment (LCA)  
85 study suggested that they are indeed an environmentally sustainable wastewater  
86 treatment technology [33]. Larger constructed METland designs are currently treating  
87 wastewater from a Camping site for 1000 inhabitants (Los Escullos, Spain) in just 50  
88 m<sup>2</sup> while fulfilling all demanding discharge limits of a Natural Park. However,

89 regardless of its high footprint efficiency, exploring new configurations of this novel  
90 technology is a must.

91 In this context, the concept of modular constructed wetlands (MTWs) emerges as  
92 an innovative enhancement upon conventional treatment wetland (TW) systems,  
93 embodying a strategic adoption of pre-designed and pre-fabricated modular units to  
94 rapidly build the wetland system and augment wastewater treatment ability [34]. The  
95 predefined modules, constructed from robust materials such as wooden or plastic, are  
96 meticulously designed to host specific substrates per unit, wetland vegetation, and  
97 microbial communities, thereby simulating natural wetland processes for wastewater  
98 purification in a more controlled and efficient manner. The inherent modularity and  
99 scalability of MTWs demonstrate superior adaptability, especially in contexts  
100 constrained by construction limitations or diverse treatment requisites, offering a  
101 symbiotic blend of physical filtration, biological degradation, and chemical  
102 transformations to synergistically mitigate pollutant concentrations in wastewater.  
103 Similar to traditional TWs, MTWs utilize specific substrate as a pivotal component to  
104 enhance pollutant removal efficiency [35], or even nutrient recovery by Wei et al.,  
105 (2024) from wastewater [36].

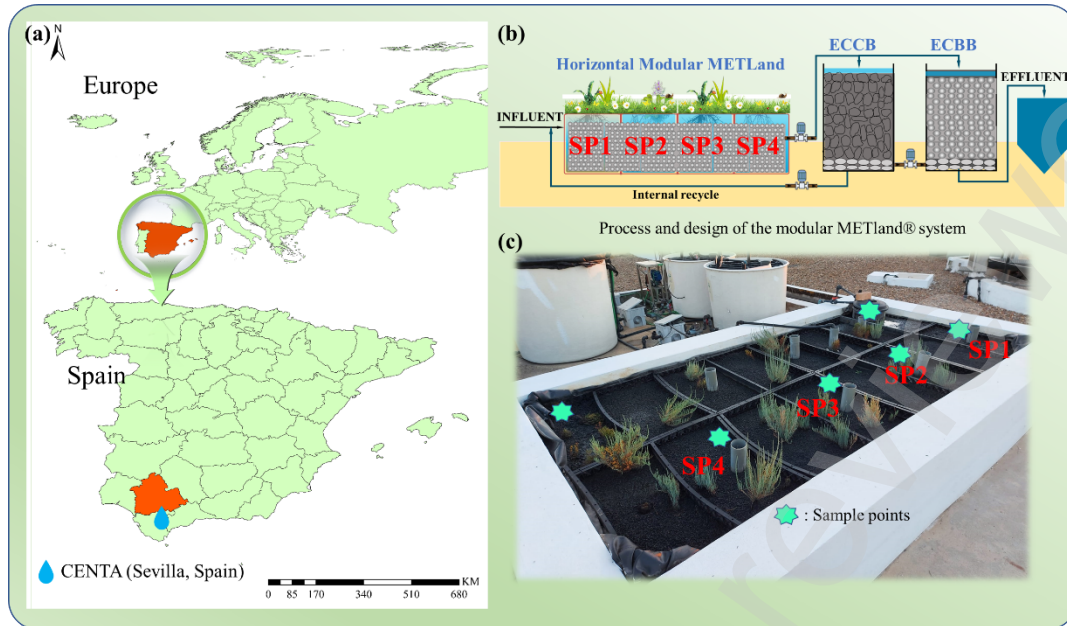
106 The objective of this study was to validate for first time modular concepts with  
107 METland® technology to implement a demo scale of modular METland® for treating  
108 real domestic wastewater treatment. This novel strategy will create new solutions to  
109 enhance the ability to effectively treat real wastewater and explore the applicated

110 possibility for different communities or regions by the scalability and design  
111 optimization of the system.

## 112 **2 Materials and methods**

### 113 ***2.1 Site description***

114 The modular METland<sup>®</sup> units were built in hybrid system, and located in the  
115 Foundation Centre for New Water Technologies (CENTA) at Carrion de Los Céspedes,  
116 (Sevilla, Spain) (Fig. 1(a)). The province of Sevilla is the western area of the  
117 Autonomous Community of Andalusia. Meanwhile, Seville has a warm Mediterranean  
118 climate with an annual average temperature of 18.5 °C. Winters are generally mild  
119 while summers are hot. The maximum temperatures in summer often surpass 40 °C  
120 [37]. This scientific centre of CENTA stands as a pivotal research institution in the field  
121 of water/wastewater technologies, and it has 41,000 m<sup>2</sup> area for experimental treatment  
122 plant that exemplifies the fusion of cutting-edge and natural water treatment systems.  
123 Integral to CENTA's mission is the real-world validation of water treatment solutions.  
124 Before entering the market, a multitude of on-site water treatments, tailored for both  
125 individual households and smaller communities, undergo rigorous testing and  
126 verification at the facility. Moreover, this extensive technological platform serves as  
127 the nexus for research endeavors undertaken by CENTA and offers collaboration  
128 opportunities for other scientific entities and corporations in the water sector.



129

130 Fig. 1 Modular METland® system in the study: (a) Location map of site; (b) Process  
 131 and operation of the system; (c) The *in situ* photograph of the system

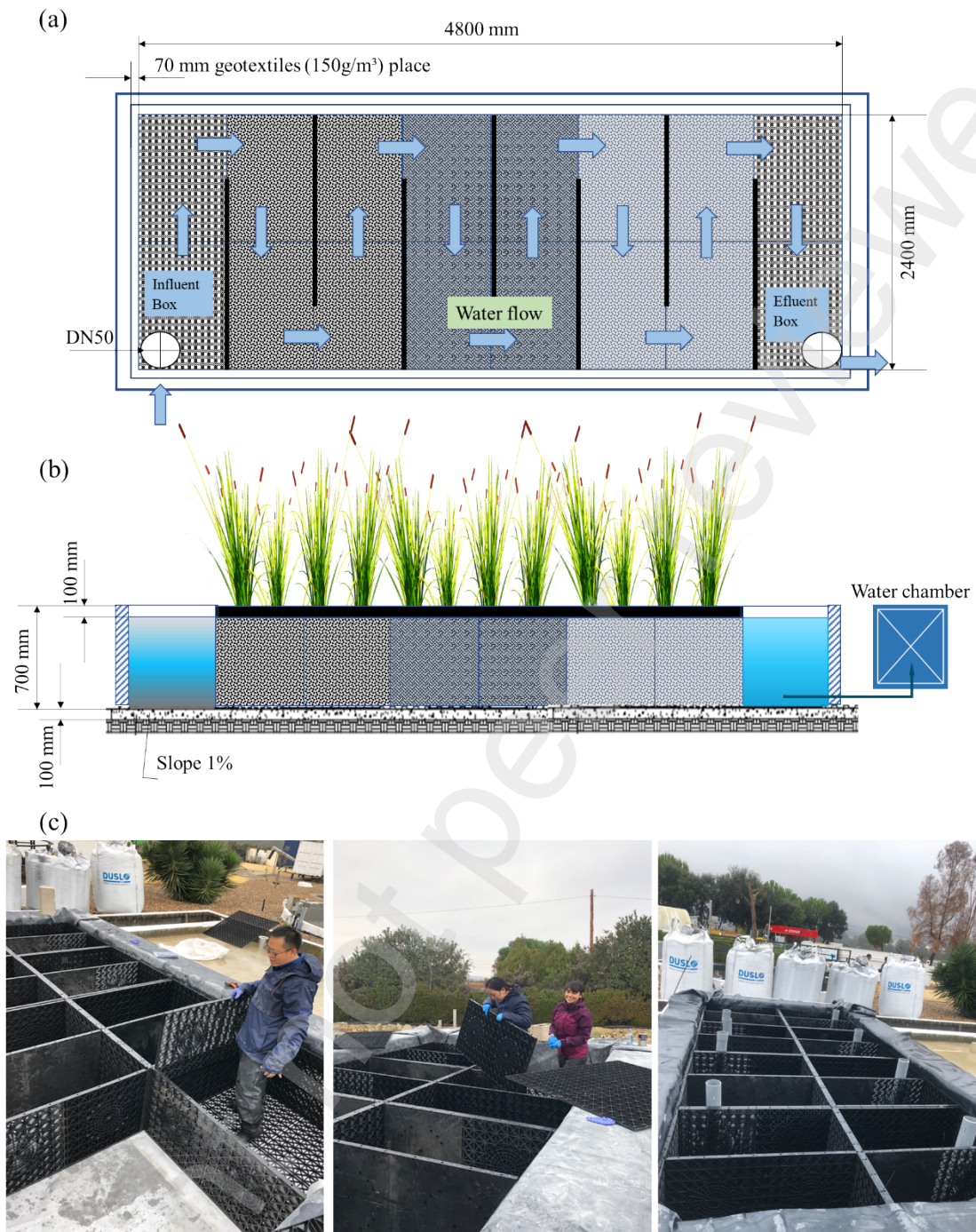
## 132 2.2 Designation, construction and operation of the overall treatment system

133 The process of the modular METland® system is shown in Fig. 1(b). It was operated in  
 134 combination with consisted of a three stages solution: i) horizontal flow  
 135 electroconductive MTW (HF-EC-MTW), ii) vertical downflow EC coke-based biofilter  
 136 (ECCB) and iii) EC biochar-based biofilter (ECBB), built in the year of 2020 at CENTA  
 137 to treat real domestic wastewater (Fig. 1(b&c)).

138 The worktable dimension of the modular METland® system is 4.8m in length,  
 139 2.4m in width, and 0.6m in depth (with the volume and the surface area are 6.91m<sup>3</sup> and  
 140 11.52 m<sup>2</sup>, respectively), and the main structures were installed by 16 plastic modules  
 141 with both solid and hollow pieces of plastic boards. The detail of the plastic modules  
 142 can be referred to Wei et al., (2024) [38]. The CAD drawing of the system is shown in  
 143 Fig. 2a,b. Additionally, the concrete brick walls were built as the external

144 reinforcements for adequate support. The bed of the modular METland® system was  
145 filled with 0.5m-deep electroconductive coke supplied by METfilter (Spain), and 5 cm  
146 of gravel at the bottom, engulfing the drainage system via Ø75 mm PVC perforated  
147 pipes. The sampling points were distributed over the system by Ø75 mm PVC  
148 perforated pipes for monitoring both water quality and bioelectrochemical activities.  
149 The schematic diagram for water flow path of the modular METland® system is shown  
150 in Fig. 2(a,b), while the *in situ* assembling scenario is shown in Fig. 2(c) .





151

152 Fig. 2 Design and assembling of the modular METland®: (a) Top view; (b) Profile view;

153 and (c) the *in situ* assembling scenario

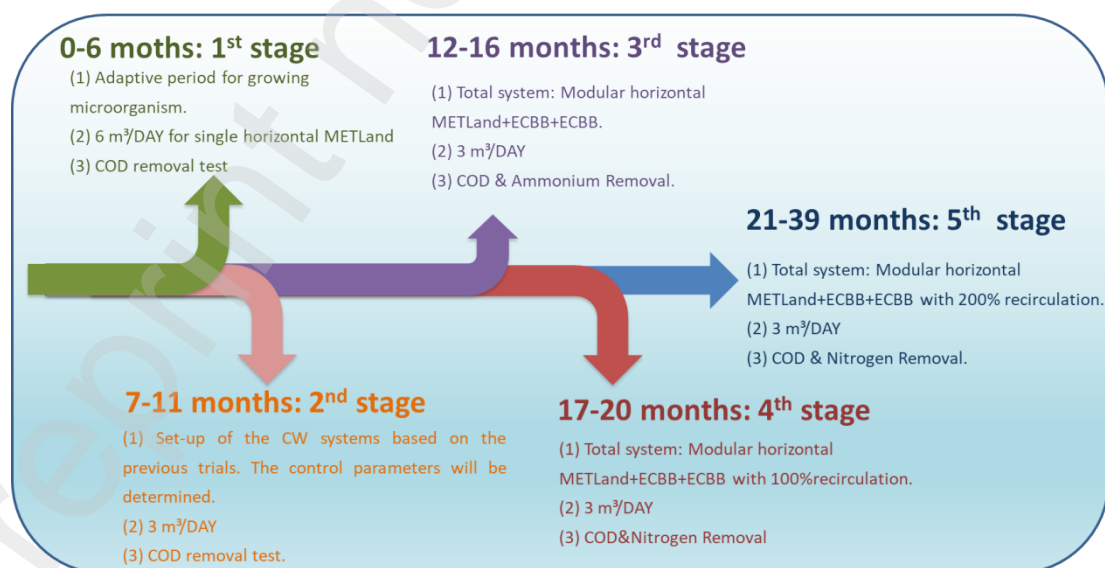
154

155 The dimensions of the additional biofilters were 1.5 m in diameter and 1.1 m in

156 height, the surface area and the volume of each biofilter were ca. 1.7 m<sup>2</sup> and 1.9 m<sup>3</sup>,

157 respectively. Both the biofilters were filled with about 10-15cm (in height) gravel in  
 158 bottom layer as foundation, then filled with electroconductive coke in ECCB and  
 159 electroconductive biochar in ECBB, respectively, as main filter medium. The two  
 160 biofilters were parallelly implemented in downflow mode after the modular METland®  
 161 unit (Fig. 1(b)).

162 The modular METland® system was operated with real domestic wastewater after  
 163 pre-treatment of septic tank. The purpose and the conditions of the operational  
 164 processes were divided into five stages (Fig. 3). The first and second stages  
 165 corresponded with 6 and 3 m<sup>3</sup>/day of flow rates, respectively, for exploring the  
 166 influence of hydraulic loading in the modular METland® system. In the third stage, two  
 167 parallel biofilters (ECCB and ECBB) are connected after modular METland® system  
 168 for considering the further treatment of ammonium. In the fourth and fifth stages, 100%  
 169 and 200% rate of effluent recirculation, respectively, from ECCB to the modular  
 170 METland® system were implemented for enhancing the TN removal.



171

172 Fig. 3 The operational conditions in the overall trial period

### 173 ***2.3 Water source, sampling and water quality analyses***

174 Urban wastewater source in continuous flow was from the municipality of Carrión de  
175 los Céspedes (2,500 inhabitants; Seville, Spain). The average pollutants concentration  
176 of wastewater were as follows: COD,  $\text{NH}_4^+$  and TN were  $419 \pm 54.1$ ,  $61.3 \pm 5.34$  and  
177  $63.4 \pm 5.28$ , respectively. According to the wastewater quality, the influent corresponds  
178 to typical urban wastewater from a small agglomeration [39].

179 The water samples from influent and effluent chambers were taken weekly after 6  
180 months of an initial acclimation period. The steady state was defined as constant  
181 removal efficiencies for pollutants without overflow and clogging events, using a flow  
182 rate of 2-3  $\text{m}^3$  per day. All the water samples were filtered and a completely physical-  
183 chemical analysis was performed by the Analytical Lab Service from CENTA, Sevilla,  
184 Spain. COD analysis was carried out by photometric evaluation (Hach LCK cuvette test  
185 + DR 3900 spectrophotometer).  $\text{NH}_4^+$ ,  $\text{NO}_3^-$  and TN were measured with photometric  
186 evaluation (Hach APC and LCK cuvette test + DR 3900 spectrophotometer).

### 187 ***2.4 Electric potential measurement to monitor in situ microbial electrochemical*** 188 ***activity***

189 To evaluate the microbial electrochemical activity of the modular METland<sup>®</sup> system,  
190 EP sensors made of shielded silver/silver chloride (Ag/AgCl) were used. Construction  
191 of such custom-made sensor were inspired by previous design reported elsewhere by  
192 Damgaard et al., (2014) [40]. The sensors, with dimensions of 0.12 cm in diameter and  
193 60 cm in height, were meticulously crafted to remain insensitive to redox-active

194 compounds. The sensors with two electrodes were placed in different measuring spots  
195 in each plastic sampling column of the system, while the electrodes were connected by  
196 voltmeter. EP readings were taken every 1cm increments at a resolution of  $\pm 45$   
197 seconds, and recorded for a duration of 30 seconds per spot [31,41]. To ease the  
198 graphical representation, the EP values (mV) were normalized using, as reference  
199 electrode, the water/atmosphere interface (0 mV at 0-cm depth). This adjustment  
200 rendered the EP profiles relative to the overlying water's potential, which served as a  
201 normalization reference. Comprehensive analyses of the EC-MCW systems' microbial  
202 electrochemical activity were then deduced from these EP measurements, along with  
203 estimations of ionic current densities (J) for forecasting the electron transfer activities.

204 The pollutants removal efficiency (RE, %) of the system was typically calculated  
205 as Eq. (1), and mass removal rate (MRR, g/m<sup>2</sup>·day) was calculated as Eq. (2), where,  
206  $C_{IN}$ ,  $C_{OUT}$ , A and Q correspond to the pollutant concentrations of influent, effluent  
207 (mg/L), surface area (m<sup>2</sup>), and flow rate (m<sup>3</sup>/day), respectively:

$$208 \quad RE = \frac{C_{IN} - C_{OUT}}{C_{IN}} \times 100\% \quad (1)$$

$$209 \quad MRR = \frac{C_{IN} - C_{OUT}}{A} \times Q \quad (2)$$

210 The ionic current density was calculated with the Ohm's Law as Eq. (3) [42]:

$$211 \quad J = -\sigma \times \frac{d\phi}{dz} \quad (3)$$

212 Where,  $J$  and  $\sigma$  represent the electron current density (A/m<sup>2</sup>) and water electrical  
213 conductivity (S/m), respectively, and  $\frac{d\phi}{dz}$  is the EP gradient (V/m).

214

## 215 **3 Results and Discussion**

### 216 **3.1 Overall performance of modular METland® system for treating real urban** 217 **wastewater**

218 An electroconductive treatment wetland, so-called METland was design and  
219 constructed for the first time following a modular strategy for treating real urban  
220 wastewater while monitoring bioelectrochemical performance by means of electric  
221 potential profile and current density. The new configuration was designated as  
222 electroconductive modular treatment wetland (EC-MTW), and it was operated for two  
223 years along five stages for achieving a robust purification of pollutants removal (Fig.  
224 3). i) The first and second stages were implemented in a range of 3-6 m<sup>3</sup>/day of flow  
225 rates for exploring the influence of hydraulic loading in MCW unit; ii) in a third stage,  
226 two parallel downflow electroconductive biofilters: EC coke-based biofilter (ECCB)  
227 and EC biochar-based biofilter (ECBB) were operated after EC-MTW unit for  
228 promoting ammonium oxidation. Finally, iii) 100% and 200% rates of recirculation  
229 from ECCB to MCW were implemented for enhancing the TN removal in the fourth,  
230 and fifth stages, respectively.

#### 231 *3.1.1 COD removal performance*

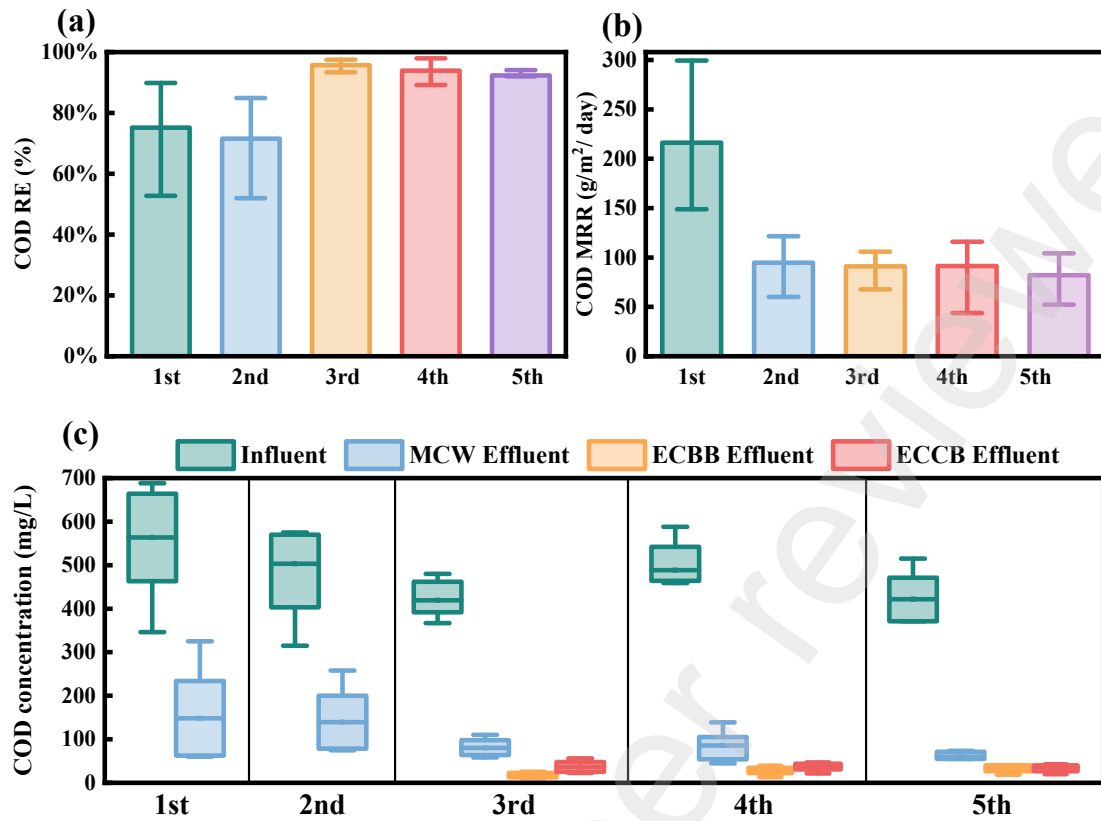
232 In order to evaluate the performance of the EC-MTW in terms of removal efficiency  
233 (RE, %), and COD removal rate (MRR, g/m<sup>2</sup>/ day), the systems were fed with a real  
234 URBAN wastewater under a continuous mode (Figure 4) Conventional horizontal  
235 subsurface flow treatment wetland (HSSF-CW) typically are designed to 3-5 m<sup>2</sup> per

236 person equivalent (pe), while in this study, the hydraulic loading of EC-MTW system  
237 were significantly high ( $6 \text{ m}^3/\text{day}$ ), leading to footprint requirements in a  $0.6 \text{ m}^2/\text{pe}$   
238 range. In the first and second stages with a single EC-MTW unit, the COD average  
239 removal rate was above 70%. Furthermore, the decrease in the second stage was  
240 attributed to a 50% reduction in flow rate. In the first two stages, the single EC-MTW  
241 unit revealed cod removal rates in the range of  $200 \text{ g/m}^2$  per day leading to effluents  
242 with ca. 140 ppm COD. This value is consistent with removal rates observed  
243 elsewhere using wastewater from the same facility (Aguirre-Sierra et al., 2016). This is  
244 remarkable considering that EC-MTW was operating at TRH 20-fold higher than  
245 standard HSSF-CW demand for treating urban wastewater. To further enhance quality  
246 of the effluent, including the need for an extra nitrifying step, the EC-MTW was  
247 upgraded by adding two parallel downflow EC biofilters made of EC coke or EC  
248 biochar (stages 3-5).

249 Thus, this multi-biofilter hybrid system revealed COD removal efficiency above  
250 90%. In particular, during the fourth and fifth stages, the additional recirculation  
251 process was implemented and significantly increased the removal rate of COD.

252 The process of removing COD from wastewater using conductive materials such  
253 as electroconductive coke or electroconductive biochar involved a unique combination  
254 of electrochemistry and biological mechanisms. Simultaneously, the role of  
255 electroconductive materials in facilitating biological degradation comes into play. The  
256 materials provided an ideal surface for the growth and activity of electroactive bacteria,

257 a key component in the biological aspect of COD reduction [36,43]. These bacteria  
258 possess the unique ability to transfer electrons to and from the surface of substrates,  
259 biochar usually has a high surface area, porosity and a variety of functional groups on  
260 its surface, which has better electron transfer than coke and then potentially facilitates  
261 the degradation process for pollutants. Thus, the COD removal performance of ECBB  
262 was always better compared to ECCB (Fig. 5cc). Moreover, this electron transfer is  
263 vital for the oxidation-reduction reactions necessary for the removal of complex organic  
264 molecules. The conductive material serves as an electron mediator between microbial  
265 metabolism and passively-supplied oxygen, thereby optimizing the efficiency of  
266 bioremediation. Furthermore, conductive coke can exhibit catalytic properties to boost  
267 redox reactions, promoting the oxidation of organic pollutants. These species are highly  
268 reactive and play a critical role in removing persistent organic molecules that are  
269 typically resistant to biological degradation.



270

271 Fig. 4. COD removal performance of EC-MCWs in different conditions. 1<sup>st</sup>: EC-  
 272 MTW1 fed with 3 m<sup>3</sup>/day; 2<sup>nd</sup>: EC-MTW 2 fed with 6 m<sup>3</sup>/day; 3<sup>rd</sup>: EC-MTW + EC DF  
 273 corresponded to EC-MTW1 followed by ECCB and ECBB biofilters operated down in  
 274 parallel; 4<sup>th</sup> and 5<sup>th</sup>: EC-MTW1 + EC DF + RC1 and EC-MTW1 + EC DF + RC2  
 275 corresponded to 100% (4<sup>th</sup>) and (5<sup>th</sup>) 200% rate of recirculation from ECCB to EC-  
 276 MTW1.

277 *3.1.2 Nitrogen removal performance*

278 The removal of N from wastewater involves a two-stage process: nitrification and  
 279 denitrification, which mainly occur under aerobic and anoxic conditions, respectively  
 280 [44]. Our modular METland® system (EC-MTW) operated under anoxic conditions due  
 281 to its horizontal flow design, so it is not optimal for nitrification. Therefore, to enhance



282 N removal efficiency, additional vertical flow biofilters (ECCB and ECBB) were added  
 283 after the EC-MTW system to provide the oxidative conditions necessary for effective  
 284 nitrification. Then, N removal was investigated under continuous wastewater feeding  
 285 for a whole year and notable difference in efficiency was observed in the reduction of  
 286  $\text{NH}_4^+\text{-N}$  and TN levels in the effluent (Table 1).

287

288 Table 1 Removal efficiency of  $\text{NH}_4^+\text{-N}$  and TN in 3<sup>rd</sup>, 4<sup>th</sup> and 5<sup>th</sup> stages of the  
 289 treatment system

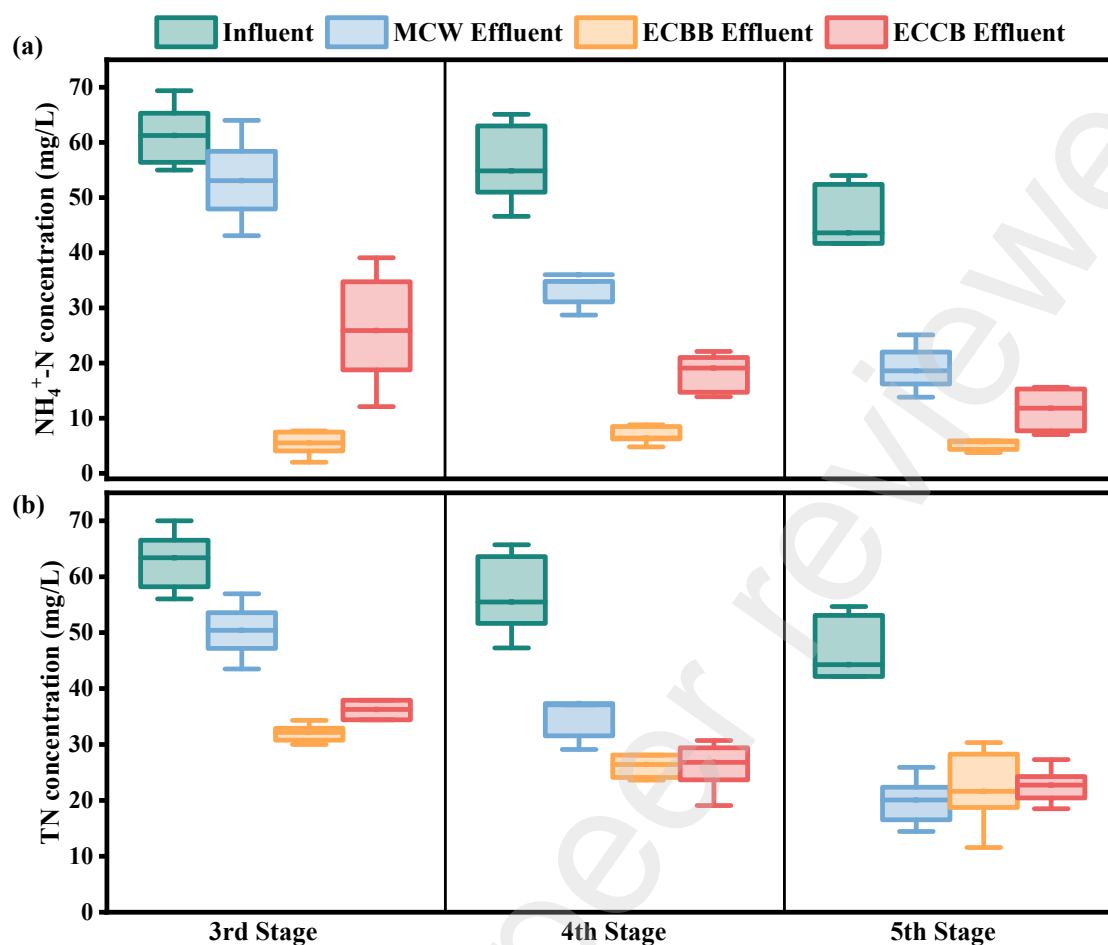
Treatment system	$\text{NH}_4^+\text{-N}$ removal efficiency (%)			TN removal efficiency (%)		
	3 <sup>rd</sup>	4 <sup>th</sup>	5 <sup>th</sup>	3 <sup>rd</sup>	4 <sup>th</sup>	5 <sup>th</sup>
EC-MTW	12.5±	31.4±	33.9±	20.0±	29.9±	31.6±
	24.6	23.9	26.8	20.3	22.2	24.3
ECCB	57.3±	62.5±	63.2±	42.8±	49.0±	46.8±
	16.4	17.3	18.1	15.6	18.3	17.1
ECBB	90.9±	87.3±	86.3±	48.9±	49.6±	45.1±
	5.62	6.82	5.17	12.8	17.8	17.2

290

291 Upon integrating the modular METland® EC-MTW with the ECCB biofilter, the  
 292  $\text{NH}_4^+\text{-N}$  removal efficiency significantly increased, starting at 57.3% in the 3<sup>rd</sup> stage  
 293 and peaking at 63.2% in the 5<sup>th</sup> stage. On top of the nitrification role, the downflow  
 294 ECCB biofilter revealed a capacity for removing total nitrogen (ca. 45%). This  
 295 unexpected result considering the inhibitory impact of oxygen on denitrification was

296 indeed previously reported [20,31], suggesting that electroconductive material may  
297 stimulate the electron transfer to nitrate in anoxic internal layers of electroactive biofilm.  
298 In contrast, the combination of modular METland® system EC-MTW with ECBB  
299 biofilter made of electroconductive biochar exhibited an even more pronounced  
300 improvement in nitrification. The effluent  $\text{NH}_4^+\text{-N}$  values from the overall treatment  
301 system drop from 53 mg/L in modular METland® system to 5.5 mg/L in ECBB unit,  
302 which can fully meet the wastewater discharge standard of Dir. 00/60/EC of 23 Oct  
303 2000 regarding ammonium (Fig. 5(a)). The system achieved a remarkable high  $\text{NH}_4^+\text{-}$   
304 N removal efficiency higher than 90% in the 3<sup>rd</sup> and 4<sup>th</sup> stages just with passive aeration  
305 and no energy cost associated with blowers. However, the effluent TN concentrations  
306 of the overall treatment system could be significantly lowered if effluent from biochar  
307 biofilter ECBB would be also recirculated. Due to management issues inside wwtp we  
308 could not perform such test. However, real METland operating in an urban wastewater  
309 (Otos municipality, Murcia, Spain) currently operates at 300% recirculation from EC  
310 downflow biofilters to successfully remove TN levels from 100ppm TN influent  
311 (Esteve-Núñez, personal communication).

312 The results clearly demonstrated that both ECCB and ECBB units significantly enhance  
313 the N removal with ECBB showing remarkable effectiveness, particularly for  $\text{NH}_4^+\text{-N}$   
314 removal.



315

316 Fig. 5  $\text{NH}_4^+\text{-N}$  (a) and TN (b) concentration for the three stages of overall treatment

317 system. 3<sup>rd</sup>: EC-MTW + EC DF corresponded to EC-MTW1 followed by ECCB and

318 ECBB biofilters operated down in parallel; 4<sup>th</sup> and 5<sup>th</sup>: EC-MTW1 + EC DF +RC1

319 and EC-MTW1 + EC DF +RC2 corresponded to 100% (4<sup>th</sup>) and (5<sup>th</sup>) 200% rate of

320 recirculation from ECCB to EC-MTW1.

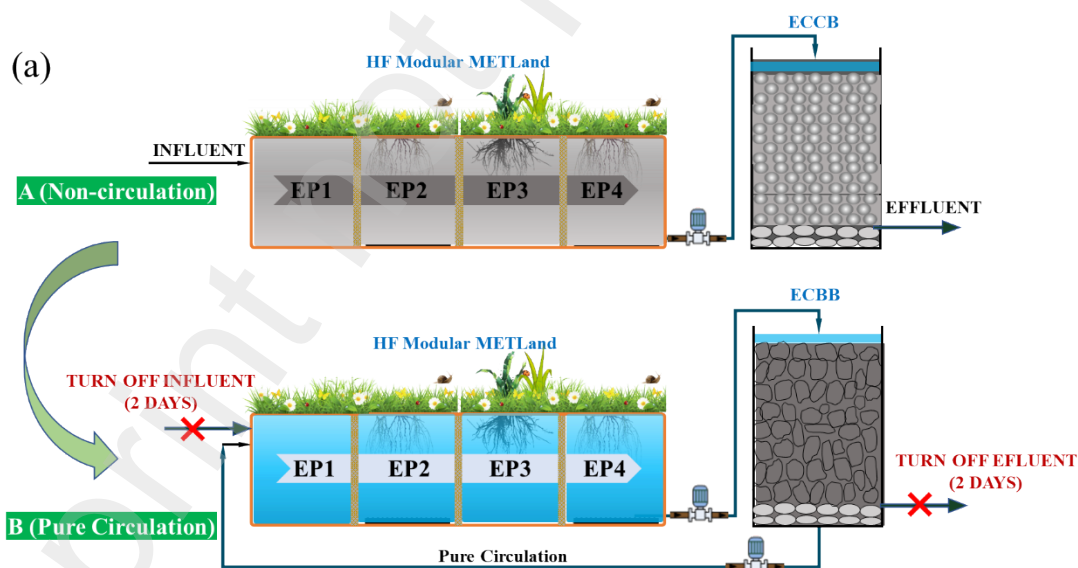
## 321 3.2 Bioelectrochemical Behavior

### 322 3.2.1 Electric potential profiles

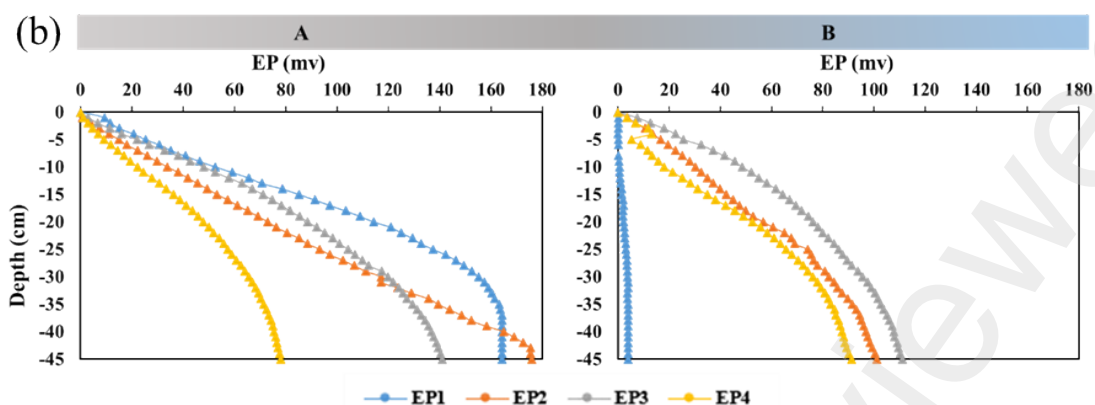
323 The design of the modular METland® (EC-MTW) consists of a single electrode, unlike

324 the traditional microbial electrochemical systems that utilize two independent

325 electrodes and an external circuit. Thus, the electrical current cannot be tested directly  
326 in this single electroconductive bed [45]. In order to gain insights into the electron flow  
327 occurring within the vertical axis of conductive substrate, an electrochemical parameter  
328 so-called electric potential (EP) was measured at this demo unit. Indeed, the electric  
329 potential profile is a useless parameter in conventional non-conductive biofilters like  
330 treatment wetlands since no variations can be monitored regarding EP [23,41]. In  
331 contrast, electron transfer along electroconductive bed from biofilters like METland®  
332 generates a measurable electric potential in the water column [31]. Thus, EP was  
333 monitored at 4 independent sampling points along the horizontal flow bed.  
334 Furthermore, EPs were monitored under two typical conditions for exploring the  
335 correlation between electroactive metabolic activity and wastewater contaminants  
336 (Figure 6).



337



338

339 Fig. 6 Electron flow along EC-MTW: (a) Operational conditions where A is continuous  
 340 mode; B is internal purely circulated mode; and and sample points (EP1, EP2, EP3,  
 341 EP4 from left to right), (b) EP profiles of tested conditions (A, B) along depth (from top)  
 342 at each sampling point

343 The horizontal subsurface flow EC-MTW system was operated under two  
 344 conditions: (A) raw wastewater under normal operational mode, (B) treated raw  
 345 wastewater under re-circulation operation. Variations in ww composition inside the bed  
 346 can be monitored through the different EP profiles (Fig. 6(b)), revealing the impact of  
 347 soluble electron acceptors (eg. nitrate or oxygen) on electron flux along the  
 348 electroconductive bed., which can eventually correlate with electroactive bacteria  
 349 capacity for removing pollutants.

350 Condition A correspond to raw wastewater, leading to higher COD concentration  
 351 (Table 2 and Fig. 7). The EP profiles in this condition revealed how electrons from  
 352 COD degradation were transferred to the EC material at 45cm depth zones and they  
 353 were eventually consumed in the upper zones where more oxidative conditions were  
 354 reached due to the presence of oxygen as electron acceptor. Such profiles were

355 measured at different locations inside the modular METland®. Under standard  
356 operation (A), the curve of EP1 location (close to influent chamber with maximum  
357 COD) revealed the max variation in mV vs height, confirming the electron transfer  
358 along bed. Electron transfer along bed is typically directly correlated with COD  
359 removal rate values because electrons are generated by microbial oxidation of COD.  
360 Such variation was diminished as far as we move away from influent (EP2 to EP4)  
361 revealing a lower electron transfer due a lower COD values at such locations. (Fig. 6).  
362 Moreover, this can serve as a strong indication of the spatial distribution changes of  
363 COD degradation in a horizontal flow METland system.

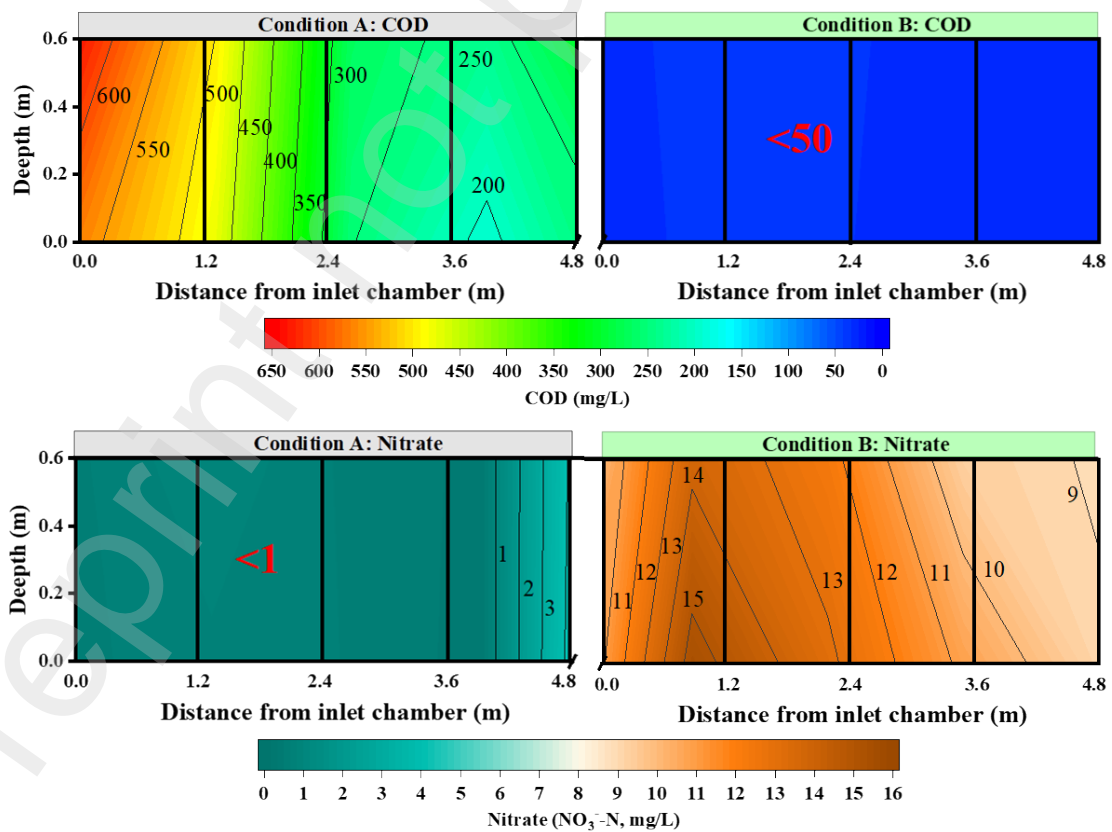
364 In order to evaluate shifts in EP in response to operation variations, a new  
365 condition B, was tested. Inflow and outflow were closed so water was recirculating  
366 between horizontal modular METland® EC-MTW and the downflow biofilter ECBC.  
367 This operational change generated the main impact at the EP1 sampling point due to  
368 the recirculation of i) oxygenated water from down-flow ECBC, and ii) 15.6ppm  
369 nitrate-containing water, both from ECBC outlet. The presence of such soluble electron  
370 acceptors (especially oxygen) should negatively alter the vertical electron flow through  
371 the bed by accepting those electrons generated in the microbial metabolism of COD  
372 even in lower zones of bed. Such hypothesis was confirmed by monitoring EP values  
373 after recirculation (Figure 6) where EP1 drastically changed after recirculation showing  
374 a flat-like appearance very similar to the one reported in gravel [23,41]. As we monitor  
375 EP away from EP1, then oxygen from recirculation stream should be consumed and

376 EP2, EP3 and EP4 recover the classical fitting of an EC bed under anoxic conditions  
 377 [31].

378 Table 2 COD and nitrate concentration in different operational conditions.

Overall treatment system	COD concentration (mg/L)		Nitrate concentration (mg/L)	
	A	B	A	B
S-EP1	565±21	36.4±3	0.62±1	15.4±1
S-EP2	476±15	34.5±8	0.79±2	13.2±2
S-EP3	252±9	28±5	0.66±1	10.8±3
S-EP4	191±14	28.5±2	0.42±1	9.09±2

379



380

381 Fig. 7 Concentration distribution of COD and Nitrate along the horizontal flow modular  
382 METland® system (EC-MTW) under continuous feeding (A) and recirculation (B)

383

384 Overall, these EP profiles served as strong evidence for spatial variations in  
385 electron utilization for pollutants degradation within a horizontal flow modular  
386 METland® system. The distinct trends under each operational condition reflect the  
387 system's dynamic response to changes in wastewater characteristics and internal  
388 processing strategies.

### 389 *3.2.2 Electron current density and response to organic pollutants*

390 In this study, horizontal flow modular METland® system was a complete electric  
391 circuit, leveraging the natural process of organic matter oxidation by electroactive  
392 bacteria [33,45]. In the system, the bacteria oxidize organic pollutants, releasing  
393 electrons that travel through an electrically conductive bed till they find a suitable  
394 electron acceptor to be consumed. Simultaneously, this oxidation process generates ion-  
395 flows in the water, creating currents. The electron flow through the conductive bed and  
396 the ion-flow through the water are equal in magnitude but opposite in direction [40].

397 This section mainly explored the correlations between COD and electron current  
398 density (J). Thus, under continuous feeding (condition A)— there was pure  
399 recirculation without influent and effluent due to complete internal circulation  
400 overnight—the system's COD was nearly depleted. Therefore, Condition B is not  
401 considered suitable for establishing a correlation between COD and J in this part of the



402 study. But this observation underlines that, despite the absence of COD under Condition  
 403 B, there might still exist a notable correlation between nitrate (N) concentration and  $J$ ,  
 404 necessitating further research. Moreover, this suggests a competitive relationship  
 405 between nitrate and electroconductive bed for accepting electrons from COD which  
 406 needs additional investigation to fully understand the dynamics of pollutant removal  
 407 and electrochemical activity within CW systems.

408 Thus, the two most commonly used operational conditions (non-recirculation or  
 409 recirculation with both influent and effluent) were studied in this section (Figure 8).  
 410 Electron current density ( $J$ ) in the system was calculated by the gradient of EP profiles  
 411 and wastewater conductivity in four sample points (Table 3). These two typical  
 412 operational scenarios were involved to investigate the characteristic variations in  
 413 electron current density ( $J$ ) and to elucidate the linear correlation between  
 414 electrochemical indices and changes in pollutant levels.

415

416 Table 3 Water conductivity ( $\sigma$ ) of each chambers in two commonly used operational  
 417 conditions.

Water conductivity ( $\mu\text{S}/\text{cm}$ )	S-EP1	S-EP2	S-EP3	S-EP4
Non-recirculation	1112	983	922	871
Recirculation	994	794	774	748

418

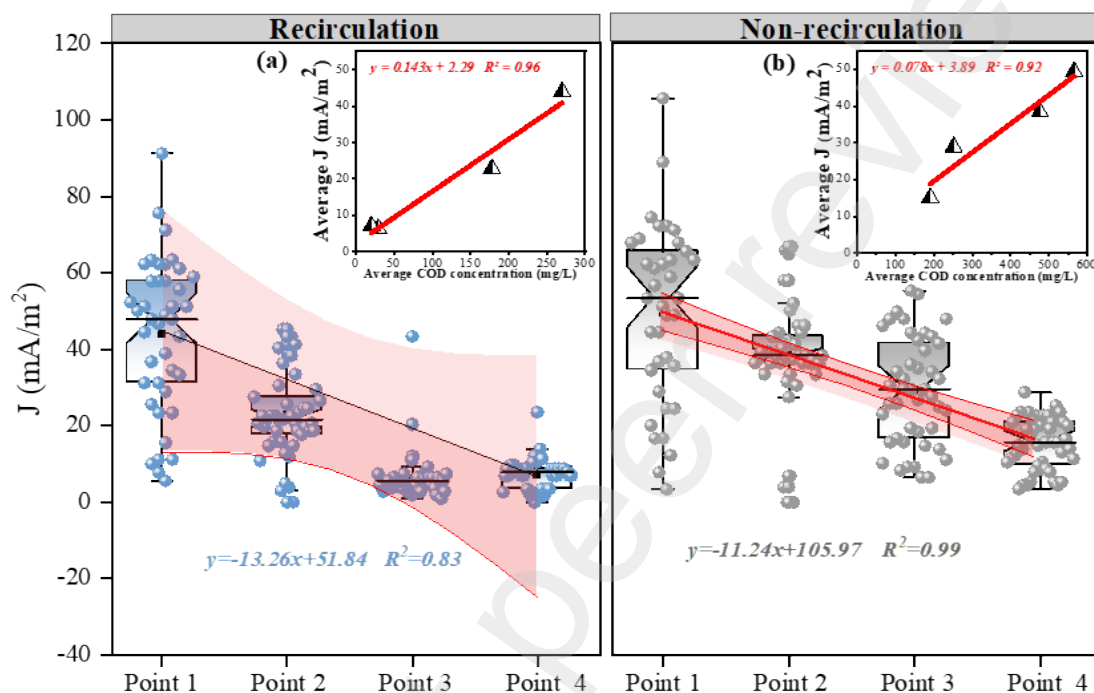
419       The J values distribution at four sampling points were calculated in the presence  
420 and in absence of recirculation (Fig. 8). In the horizontal flow modular METland®  
421 system, J values were generally decreasing from the sampling point near the water inlet  
422 chamber (S-EP1) to the sampling point near the water outlet chamber (S-EP4) under  
423 both recirculation and non-recirculation conditions. The J values for the recirculation  
424 condition decreased from inlet zone ( $J=43.99 \text{ mA/m}^2$ ) to outlet zone ( $J=7.08 \text{ mA/m}^2$ ),  
425 and from 49.38 to 15  $\text{mA/m}^2$  for the non-recirculation conditions. For a CW treatment  
426 system to daily treat a large volume of influent wastewater, recirculating the effluent is  
427 highlighted as a routine yet effective operational strategy to enhance the efficiency of  
428 pollutant removal. The systems with recirculation in place generally exhibit a  
429 substantial reduction in the overall concentrations of pollutants compared to those  
430 without recirculation [46]. In this study, the pollutant concentrations, such as COD,  
431 ranged from 20-270 mg/L under recirculation conditions. This is significantly lower  
432 than the COD concentrations under non-recirculating conditions, which ranged from  
433 191-565 mg/L. This significant variability not only points to the efficacy of  
434 recirculation in pollutant reduction, the feedback effect can also be seen in the  
435 distribution curve of the current density J. Under recirculation conditions, with lower  
436 COD levels, the overall average distribution value of J is significantly lower than that  
437 under non-recirculating conditions (higher COD values). Moreover, this positive  
438 correlation trend is also evident in the horizontal flow wetland from the inlet to the  
439 outlet. This correlation is consistently observable along the flow path of the wetland, as

440 the concentration of pollutants decreases from the inlet to the outlet, the J value  
441 distribution also decreases and shows a linear relationship.

442 Indeed, the J values in this study were generally lower than previously reported in  
443 non-modular METlands® (ranging from 45.09 to 223.84 mA/m<sup>2</sup>) [31]. The main  
444 reason of such discrepancy could be due to the different feeding patterns between both  
445 studies: down-flow subsurface feeding distributed along the whole METland surface  
446 [31] versus standard horizontal subsurface flow where feeding occurs in a single point  
447 (this study). Such different feeding profiles would generate a totally different scenario  
448 regarding COD distribution and microbial activity so it is reasonable to observe a  
449 different electron flow profile along surface.

450 The linear regression results suggest a good fit for the J value change in relation  
451 to the position within the EC-MTW, with R<sup>2</sup> values of 0.83 for recirculation and 0.99  
452 for non-recirculation conditions. This indicated a strong correlation between the  
453 electrochemical indicators and the wastewater treatment process, where the electric  
454 current decreased as wastewater progressed through the system. The analysis further  
455 correlated the average COD concentration at each sampling point with the average J  
456 values, exploring the relationship between organic pollutant load and electrochemical  
457 activity. This relationship was supported by R<sup>2</sup> values of 0.96 for recirculation and 0.92  
458 for non-recirculation conditions, which indicates a strong correlation (Figure 8). The  
459 linear relationship between the COD removal and the J values throughout the system  
460 not only demonstrates the effectiveness of recirculation but also highlights the  
461 predictable nature of the treatment efficacy from the water inlet to the outlet in the EC-

462 MTW. Such clear linear relationships may provide significant evidence that can be used  
 463 to indicate pollutant concentrations through electrochemical indicators in future system  
 464 operations.  
 465



466  
 467 Fig. 8 Bioelectrochemical response through current density  $J$  ( $\text{mA}/\text{m}^2$ ) for horizontal  
 468 flow EC-MTW system under (a) recirculation (b) non-recirculation

### 469 3.2.3 Perspective and recommendations based on electrochemical behavior

470 The investigation of EP and  $J$  across different sections of the modular METland® EC-  
 471 MTW provides invaluable insights for design optimization. For instance, areas with  
 472 higher electron utilization, as indicated by steeper EP gradients, suggest more active  
 473 microbial degradation of pollutants. This understanding can guide the strategic  
 474 placement and proportion of electroconductive substrates in various sections of the  
 475 MCW. Optimizing the ratio of conductive substrate in the relatively active zone of

476 system, based on the observed electric behavior, can enhance overall treatment  
477 efficiency. More significantly, the modular nature of the system allows for tailored  
478 configurations to suit specific treatment requirements, ensuring that each module is  
479 optimally designed for its role in the treatment process.

480 J is a critical indicator of microbial activity within the system. Observations of  
481 decreasing J values along the flow path indicate areas where organic matter oxidation  
482 is more pronounced. This information is pivotal in determining the HRT and flow rates  
483 of the modular METland® system, ensuring that wastewater remains in high-activity  
484 areas for optimal treatment time although flow rate seems not significantly impact the  
485 treatment efficiency in the current study. No doubt, adjusting the flow rate to maintain  
486 the balance between sufficient contact time for microbial action and efficient  
487 throughput can improve the system's performance. Furthermore, the EP measurements  
488 can inform the frequency and extent of recirculation within the system, which is crucial  
489 for enhancing N removal efficiency.

490 Understanding the electric behavior within the modular METland® system opens  
491 avenues for enhancing its sustainability and scalability. By identifying the most  
492 efficient substrate composition and arrangement through electric behavior analysis, the  
493 system's footprint can be minimized without compromising treatment efficiency. This  
494 aspect is particularly beneficial for scaling the system up for urban applications or down  
495 for rural settings. Additionally, insights gained from electric behavior studies can guide  
496 the development of more energy-efficient systems, potentially integrating with

497 renewable energy sources, thereby contributing to the overall sustainability of  
498 wastewater treatment infrastructures.

#### 499 **4 Conclusions**

500 The integration of electric conductive substrates within the horizontal flow MCW,  
501 connecting with both coke and biochar-based downflow biofilters in a hybrid system,  
502 has demonstrated a sustainable and efficient removal of pollutants. This system  
503 leveraged electrobioremediation field , utilizing the conductive properties of materials  
504 to enhance the metabolic processes of electro-active microbes, thereby facilitating  
505 increased degradation of organic pollutants and nitrogen compounds. Moreover, this  
506 study confirms that the J within the horizontal flow modular METland® system  
507 decreases along the flow path from the inlet to the outlet, suggesting a consistent  
508 electrochemical activity that aligns with the treatment process. Overall, the findings  
509 from this study underscore the potential of modular METland® system as a scalable  
510 and effective solution for wastewater treatment in various operational processes,  
511 providing a foundation for further exploration and optimization of these systems in real-  
512 world applications.

513

#### 514 **Acknowledgements**

515 This study was supported by the Spanish Ministry of Science through Innovation with  
516 the research project “mobiMET” (grant number CPP2021-008936).

517

518

519

520

521

522

523

## 524 References

- 525 [1] G. Libralato, A. Volpi Ghirardini, F. Avezzi, To centralise or to decentralise: An  
526 overview of the most recent trends in wastewater treatment management, *J.*  
527 *Environ. Manage.* 94 (2012) 61–68.  
528 <https://doi.org/10.1016/j.jenvman.2011.07.010>.
- 529 [2] M. Scholz, Special Issue on Treatment Wetlands, *Environments* 8 (2021) 30.  
530 <https://doi.org/10.3390/environments8040030>.
- 531 [3] H. Chen, B. Gao, Y. Guo, Q. Yu, M. Hu, X. Zhang, Adding carbon sources to the  
532 substrates enhances Cr and Ni removal and mitigates greenhouse gas emissions in  
533 constructed wetlands, *Environ. Res.* 252 (2024) 118940.  
534 <https://doi.org/10.1016/j.envres.2024.118940>.
- 535 [4] D. Kotsia, T. Sympikou, E. Topi, F. Pappa, C. Matsoukas, M.S. Fountoulakis, Use  
536 of recycled construction and demolition waste as substrate in constructed wetlands  
537 for the wastewater treatment of cheese production, *J. Environ. Manage.* 362 (2024)  
538 121324. <https://doi.org/10.1016/j.jenvman.2024.121324>.
- 539 [5] Y.-R. Zhang, J.-M. Xu, H.-R. Xu, G.-D. Zhang, X.-B. Liu, H.-Y. Cheng, Insights  
540 into the response of nitrogen metabolism to sulfamethoxazole contamination in  
541 constructed wetlands with varied substrates, *Bioresour. Technol.* 397 (2024)  
542 130482. <https://doi.org/10.1016/j.biortech.2024.130482>.
- 543 [6] L. Bolton, S. Joseph, M. Greenway, S. Donne, P. Munroe, C.E. Marjo, Phosphorus  
544 adsorption onto an enriched biochar substrate in constructed wetlands treating  
545 wastewater, *Ecol. Eng.* 142 (2019) 100005.  
546 <https://doi.org/10.1016/j.ecoena.2019.100005>.
- 547 [7] Z. Cao, L. Zhou, Z. Gao, Z. Huang, X. Jiao, Z. Zhang, K. Ma, Z. Di, Y. Bai,  
548 Comprehensive benefits assessment of using recycled concrete aggregates as the  
549 substrate in constructed wetland polishing effluent from wastewater treatment  
550 plant, *J. Clean. Prod.* 288 (2021) 125551.  
551 <https://doi.org/10.1016/j.jclepro.2020.125551>.
- 552 [8] S. Gray, J. Kinross, P. Read, A. Marland, The nutrient assimilative capacity of  
553 maerl as a substrate in constructed wetland systems for waste treatment, *Water*  
554 *Res.* 34 (2000) 2183–2190. [https://doi.org/10.1016/S0043-1354\(99\)00414-5](https://doi.org/10.1016/S0043-1354(99)00414-5).
- 555 [9] T. Saeed, M. Jihad Miah, Organic matter and nutrient removal in tidal flow-based  
556 microbial fuel cell constructed wetlands: Media and flood-dry period ratio, *Chem.*  
557 *Eng. J.* 411 (2021) 128507. <https://doi.org/10.1016/j.cej.2021.128507>.
- 558 [10] S. Mosquera-Romero, E. Ntagia, D.P.L. Rousseau, A. Esteve-Núñez, A. PrévotEAU,  
559 Water treatment and reclamation by implementing electrochemical systems with  
560 constructed wetlands, *Environ. Sci. Ecotechnology* 16 (2023) 100265.  
561 <https://doi.org/10.1016/j.ese.2023.100265>.
- 562 [11] M.G. Salinas-Juárez, S.I. Ortiz-Zamora, P. Roquero-Tejeda, F.J. Garfias-Vásquez,  
563 M. del C. Durán-Domínguez-de-Bazúa, Evaluation of electrode separators and the  
564 external resistance in electrochemically assisted constructed wetlands, *Taylor*  
565 *Francis* (2024).  
566 <https://www.tandfonline.com/doi/abs/10.1080/15226514.2024.2325569>

- 567 (accessed August 5, 2024).
- 568 [12] C. Corbella, M. Guivernau, M. Viñas, J. Puigagut, Operational, design and  
569 microbial aspects related to power production with microbial fuel cells  
570 implemented in constructed wetlands, *Water Res.* 84 (2015) 232–242.  
571 <https://doi.org/10.1016/j.watres.2015.06.005>.
- 572 [13] H. Zhu, T. Niu, B. Shutes, X. Wang, C. He, S. Hou, Integration of MFC reduces  
573 CH<sub>4</sub>, N<sub>2</sub>O and NH<sub>3</sub> emissions in batch-fed wetland systems, *Water Res.* 226  
574 (2022) 119226. <https://doi.org/10.1016/j.watres.2022.119226>.
- 575 [14] A. Ebrahimi, M. Sivakumar, C. McLauchlan, A. Ansari, A.S. Vishwanathan, A  
576 critical review of the symbiotic relationship between constructed wetland and  
577 microbial fuel cell for enhancing pollutant removal and energy generation, *J.*  
578 *Environ. Chem. Eng.* 9 (2021) 105011. <https://doi.org/10.1016/j.jece.2020.105011>.
- 579 [15] Y. Huang, Y. Zhao, C. Tang, A.K. Yadav, R. Abbassi, P. Kang, Y. Cai, A. Liu, A.  
580 Yang, M. Li, A glance of coupled water and wastewater treatment systems based  
581 on microbial fuel cells, *Sci. Total Environ.* 892 (2023) 164599.  
582 <https://doi.org/10.1016/j.scitotenv.2023.164599>.
- 583 [16] X. Huang, C. Duan, W. Duan, F. Sun, H. Cui, S. Zhang, X. Chen, Role of electrode  
584 materials on performance and microbial characteristics in the constructed wetland  
585 coupled microbial fuel cell (CW-MFC): A review, *J. Clean. Prod.* 301 (2021)  
586 126951. <https://doi.org/10.1016/j.jclepro.2021.126951>.
- 587 [17] V. Kiran Kumar, K. Man mohan, S.P. Manangath, S. Gajalakshmi, Innovative  
588 pilot-scale constructed wetland-microbial fuel cell system for enhanced  
589 wastewater treatment and bioelectricity production, *Chem. Eng. J.* 460 (2023)  
590 141686. <https://doi.org/10.1016/j.cej.2023.141686>.
- 591 [18] H. Xin, R. Yang, C. Lin, J. Zhan, Q. Yang, Packing blockage and power generation  
592 of constructed wetland coupled microbial fuel cell systems using biochar as  
593 electrode and filler with different ratios, *Chem. Eng. J.* 488 (2024) 150978.  
594 <https://doi.org/10.1016/j.cej.2024.150978>.
- 595 [19] A. Aguirre-Sierra, T. Bacchetti-De Gregoris, A. Berná, J.J. Salas, C. Aragón, A.  
596 Esteve-Núñez, Microbial electrochemical systems outperform fixed-bed biofilters  
597 in cleaning up urban wastewater, *Env. Sci Water Res Technol* 2 (2016) 984–993.  
598 <https://doi.org/10.1039/C6EW00172F>.
- 599 [20] A. Aguirre-Sierra, T.B.-D. Gregoris, J.J. Salas, A. de Deus, A. Esteve-Núñez, A  
600 new concept in constructed wetlands: assessment of aerobic electroconductive  
601 biofilters, (n.d.). <https://doi.org/10.1039/C9EW00696F>.
- 602 [21] C.A. Ramírez-Vargas, C.A. Arias, P. Carvalho, L. Zhang, A. Esteve-Núñez, H.  
603 Brix, Electroactive biofilm-based constructed wetland (EABB-CW): A  
604 mesocosm-scale test of an innovative setup for wastewater treatment, *Sci. Total*  
605 *Environ.* 659 (2019) 796–806. <https://doi.org/10.1016/j.scitotenv.2018.12.432>.
- 606 [22] A. Prado, C.A. Ramírez-Vargas, C.A. Arias, A. Esteve-Núñez, Novel  
607 bioelectrochemical strategies for domesticating the electron flow in constructed  
608 wetlands, *Sci. Total Environ.* 735 (2020) 139522.  
609 <https://doi.org/10.1016/j.scitotenv.2020.139522>.
- 610 [23] A. Prado, R. Berenguer, A. Esteve-Núñez, Evaluating bioelectrochemically-  
611 assisted constructed wetland (METland®) for treating wastewater: Analysis of  
612 materials, performance and electroactive communities, *Chem. Eng. J.* 440 (2022).  
613 <https://doi.org/10.1016/j.cej.2022.135748>.
- 614 [24] A. Schievano, R. Berenguer, A. Goglio, S. Bocchi, S. Marzorati, L. Rago, R.O.  
615 Louro, C.M. Paquete, A. Esteve-Núñez, Electroactive Biochar for Large-Scale  
616 Environmental Applications of Microbial Electrochemistry, *ACS Sustain. Chem.*  
617 *Eng.* 7 (2019) 18198–18212. <https://doi.org/10.1021/acssuschemeng.9b04229>.
- 618 [25] A. PrévotEAU, F. Ronsse, I. Cid, P. Boeckx, K. Rabaey, The electron donating  
619 capacity of biochar is dramatically underestimated, *Sci. Rep.* 6 (2016) 1–11.  
620 <https://doi.org/10.1038/srep32870>.
- 621 [26] P.M. Shrestha, A.-E. Rotaru, *Frontiers | Plugging in or going wireless: strategies*  
622 *for interspecies electron transfer, (n.d.).*  
623 [https://www.frontiersin.org/journals/microbiology/articles/10.3389/fmicb.2014.0](https://www.frontiersin.org/journals/microbiology/articles/10.3389/fmicb.2014.02377/full)  
624 [2377/full](https://www.frontiersin.org/journals/microbiology/articles/10.3389/fmicb.2014.02377/full) (accessed July 13, 2024).



- 625 [27] R. Ae, C. F, S. H, M. F, S. Pm, W. Hs, S.-W. Olo, H. Poj, R. Hh, M. N, T. B,  
626 Conductive Particles Enable Syntrophic Acetate Oxidation between *Geobacter*  
627 and *Methanosarcina* from Coastal Sediments, PubMed (2018).  
628 <https://pubmed.ncbi.nlm.nih.gov/29717006/> (accessed July 13, 2024).
- 629 [28] A.-E. Rotaru, N.R. Posth, C.R. Löscher, M.R. Miracle, E. Vicente, R.P. Cox, J.  
630 Thompson, S.W. Poulton, B. Thamdrup, Interspecies interactions mediated by  
631 conductive minerals in the sediments of the ferruginous Lake La Cruz, Spain,  
632 (2018). <https://doi.org/10.1101/366542>.
- 633 [29] J. Chang, Q. Wu, P. Liang, X. Huang, Enhancement of nitrite-dependent anaerobic  
634 methane oxidation via *Geobacter sulfurreducens*, *Sci. Total Environ.* 766 (2021)  
635 144230. <https://doi.org/10.1016/j.scitotenv.2020.144230>.
- 636 [30] J. Xie, X. Zou, Y. Chang, H. Liu, M.-H. Cui, T.C. Zhang, J. Xi, C. Chen, A  
637 feasibility investigation of a pilot-scale bioelectrochemical coupled anaerobic  
638 digestion system with centric electrode module for real membrane manufacturing  
639 wastewater treatment, *Bioresour. Technol.* 368 (2023) 128371.  
640 <https://doi.org/10.1016/j.biortech.2022.128371>.
- 641 [31] L. Peñacoba-Antona, C.A. Ramirez-Vargas, C. Wardman, A.A. Carmona-  
642 Martinez, A. Esteve-Núñez, D. Paredes, H. Brix, C.A. Arias, Microbial  
643 Electrochemically Assisted Treatment Wetlands: Current Flow Density as a  
644 Performance Indicator in Real-Scale Systems in Mediterranean and Northern  
645 European Locations, *Front. Microbiol.* 13 (2022).  
646 <https://doi.org/10.3389/fmicb.2022.843135>.
- 647 [32] Á. Pun, K. Boltos, P. Letón, A. Esteve-Núñez, Detoxification of wastewater  
648 containing pharmaceuticals using horizontal flow bioelectrochemical filter,  
649 *Bioresour. Technol. Rep.* 7 (2019) 100296.  
650 <https://doi.org/10.1016/j.biteb.2019.100296>.
- 651 [33] L. Peñacoba-Antona, M. Gómez-Delgado, A. Esteve-Núñez, Multi-Criteria  
652 Evaluation and Sensitivity Analysis for the Optimal Location of Constructed  
653 Wetlands (METland) at Oceanic and Mediterranean Areas, *Int. J. Environ. Res.*  
654 *Public. Health* 18 (2021) 5415. <https://doi.org/10.3390/ijerph18105415>.
- 655 [34] Y. Zhao, B. Ji, R. Liu, B. Ren, T. Wei, Constructed treatment wetland: Glance of  
656 development and future perspectives, *Water Cycle* 1 (2020) 104–112.  
657 <https://doi.org/10.1016/j.watcyc.2020.07.002>.
- 658 [35] Y. Yang, Y. Zhao, R. Liu, D. Morgan, Global development of various emerged  
659 substrates utilized in constructed wetlands, *Bioresour. Technol.* 261 (2018) 441–  
660 452. <https://doi.org/10.1016/j.biortech.2018.03.085>.
- 661 [36] T. Wei, Y. Zhao, J. Guo, B. Ji, Á.P. García, A.E. Núñez, Developing a novel  
662 lightweight substrate for constructed treatment wetland: The idea and the reality,  
663 *J. Water Process Eng.* 57 (2024) 104587.  
664 <https://doi.org/10.1016/j.jwpe.2023.104587>.
- 665 [37] Sevilla - Official Andalusia tourism website, (n.d.).  
666 <https://www.andalucia.org/en/provincia-sevilla> (accessed October 17, 2023).
- 667 [38] T. Wei, Y. Zhao, M. Zhou, Z. Zhang, Y. Wei, A.E. Núñez, Initial concept and  
668 embodiment to develop modular constructed wetland: A unique and promising  
669 solution to sustainability transitions in water management, *J. Clean. Prod.* (2024)  
670 141912. <https://doi.org/10.1016/j.jclepro.2024.141912>.
- 671 [39] (PDF) Metcalf & Eddy Wastewater Engineering Treatment and Reuse (4th edition)  
672 (2004) | Akhid Maulana - Academia.edu, (n.d.).  
673 [https://www.academia.edu/40928611/Metcalf\\_and\\_Eddy\\_Wastewater\\_Engineering\\_Treatment\\_and\\_Reuse\\_4th\\_edition\\_2004](https://www.academia.edu/40928611/Metcalf_and_Eddy_Wastewater_Engineering_Treatment_and_Reuse_4th_edition_2004) (accessed October 18, 2023).
- 674 [40] L.R. Damgaard, N. Risgaard-Petersen, L.P. Nielsen, Electric potential  
675 microelectrode for studies of electrobiogeophysics, *J. Geophys. Res.*  
676 *Biogeosciences* 119 (2014) 1906–1917. <https://doi.org/10.1002/2014JG002665>.
- 677 [41] C.A. Ramirez-Vargas, C.A. Arias, P. Carvalho, L. Zhang, A. Esteve-Núñez, H.  
678 Brix, Electroactive biofilm-based constructed wetland (EABB-CW): A  
679 mesocosm-scale test of an innovative setup for wastewater treatment, *Sci. Total*  
680 *Environ.* 659 (2019) 796–806. <https://doi.org/10.1016/j.scitotenv.2018.12.432>.
- 681 [42] N. Risgaard-Petersen, L.R. Damgaard, A. Revil, L.P. Nielsen, Mapping electron

- 683 sources and sinks in a marine biogeobattery, *J. Geophys. Res. Biogeosciences* 119  
684 (2014) 1475–1486. <https://doi.org/10.1002/2014JG002673>.
- 685 [43] A. Prado, R. Berenguer, A. Esteve-Núñez, Electroactive biochar outperforms  
686 highly conductive carbon materials for biodegrading pollutants by enhancing  
687 microbial extracellular electron transfer, *Carbon* 146 (2019) 597–609.  
688 <https://doi.org/10.1016/j.carbon.2019.02.038>.
- 689 [44] Z. Hu, H. Yao, S. Deng, C. Zhang, S. Peng, Z. Zhang, D. Li, Iron [Fe(0)]-carbon  
690 micro-electrolysis enhances simultaneous nitrogen and phosphorus removal in  
691 vertical flow constructed wetlands for advanced treatment of reclaimed water, *J.*  
692 *Environ. Manage.* 335 (2023) 117528.  
693 <https://doi.org/10.1016/j.jenvman.2023.117528>.
- 694 [45] A. Prado, C.A. Ramírez-Vargas, C.A. Arias, A. Esteve-Núñez, Novel  
695 bioelectrochemical strategies for domesticating the electron flow in constructed  
696 wetlands, *Sci. Total Environ.* 735 (2020) 139522.  
697 <https://doi.org/10.1016/j.scitotenv.2020.139522>.
- 698 [46] C. Yang, T. Fu, H. Wang, R. Chen, B. Wang, T. He, Y. Pi, J. Zhou, T. Liang, M.  
699 Chen, Removal of organic pollutants by effluent recirculation constructed  
700 wetlands system treating landfill leachate, *Environ. Technol. Innov.* 24 (2021)  
701 101843. <https://doi.org/10.1016/j.eti.2021.101843>.

702